THE JOURNAL OF EXPERIMENTAL ZOOLOGY 278:356–371 (1997)

Water Distribution and Permeability of Zebrafish Embryos, *Brachydanio rerio*

M. HAGEDORN,[1*] F.W. KLEINHANS,[2] R. FREITAS,[3] J. LIU,[2,4] E.W. HSU,[5] D.E. WILDT,[1] AND W.F. RALL[1,6]

[1]*Smithsonian Institution, National Zoological Park and Conservation and Research Center, Washington, DC 20008*

[2]*Department of Physics, Indiana University–Purdue University Indianapolis, Indianapolis, Indiana 46202*

[3]*Department of Mechanical Engineering, University of Texas, Austin, Texas 78712*

[4]*Cryobiology Research Institute, Methodist Hospital of Indiana Inc., Indianapolis, Indiana 46202*

[5]*Department of Biomedical Engineering, Johns Hopkins University School of Medicine, Baltimore, Maryland 21205*

[6]*Veterinary Resources Program, National Center for Research Resources, National Institutes of Health, Bethesda, Maryland 20892*

ABSTRACT Teleost embryos have not been successfully cryopreserved. To formulate successful cryopreservation protocols, the distribution and cellular permeability to water must be understood. In this paper, the zebrafish (*Brachydanio rerio*) was used as a model for basic studies of the distribution to permeability to water. These embryos are a complex multi-compartmental system composed of two membrane-limited compartments, a large yolk (surrounded by the yolk syncytial layer) and differentiating blastoderm cells (each surrounded by a plasma membrane). Due to the complexity of this system, a variety of techniques, including magnetic resonance microscopy and electron spin resonance, was used to measure the water in these compartments. Cellular water was distributed unequally in each compartment. At the 6-somite stage, the percent water (V/V) was distributed as follows: total in embryo = 74%, total in yolk = 42%, and total in blastoderm = 82%. A one-compartment model was used to analyze kinetic, osmotic shrinkage data and determine a phenomenological water permeability parameter, L_p, assuming intracellular isosmotic compartments of either 40 or 300 mosm. This analysis revealed that the membrane permeability changed ($P < 0.05$) during development. During the 75% epiboly to 3-somite stage, the mean membrane permeability remained constant ($L_p = 0.022 \pm 0.002$ μm x $min^{-1}atm^{-1}$ [mean ± S.E.M.] assuming isosmotic is 40 mosm or $L_p = 0.049 \pm 0.008$ μm x $min^{-1}atm^{-1}$ assuming isosmotic is 300 mosm). However, at the 6-somite stage, Lp increased twofold ($L_p = 0.040 \pm 0.004$ μm x $min^{-1}atm^{-1}$ assuming isosmotic is 40 mosm or $L_p = 0.100 \pm 0.017$ μm × $min^{-1}atm^{-1}$ assuming isosmotic is 300 mosm). Therefore, the low permeability of the zebrafish embryo coupled with its large size (and consequent low area to volume ratio) led to a very slow osmotic response that should be considered before formulating cryopreservation protocols. *J. Exp. Zool. 278:356–371, 1997.*

Since Blaxter's ('53) pioneering experiments more than four decades ago, successful cryopreservation of teleost oocytes and embryos has remained elusive. The availability of cryopreserved oocytes and embryos, however, could have a profound influence on medical research, aquaculture, and conservation biology. The ability to cryopreserve teleost cmbryos would permit the storage of a diverse gene pool, thus allowing the maintenance of valuable transgenic lines and hybrids. Moreover, the development of frozen or "insurance" populations would preserve genetic diversity and assist efforts to prevent the extinction of fish species in natural aquatic ecosystems (Ballou, '92; Wildt, '92; Wildt et al., '93). In this paper, we investigated the distribution of water and membrane permeability to water in zebrafish

*Correspondence to: M. Hagedorn, National Zoological Park, Smithsonian Institution, 3001 Conn. Ave., NW, Washington, DC 20008. Email: NZPAH008@SIVM.SI.EDU.

Received 7 November 1996; Revision accepted 28 February 1997

embryos as a first step towards successful cryopreservation protocols.

Our laboratory used the zebrafish (*Brachydanio rerio*) as a model for developing an understanding of the cryobiological properties of teleost embryos. Zebrafish are advantageous models because a substantial database on their developmental biology (Hisaoka and Battle, '58; Hisaoka and Firllit, '60; for a review see Westerfield, '93), culture in vitro (Westerfield, '93), and some published information on the permeability and toxicity of cryoprotectants already exist (Harvey and Chamberlain, '82; Harvey et al., '83; Zhang et al., '93; Zhang and Rawson, '95, '96).

Throughout most of these studies, the outer protective membrane or embryo chorion, a noncellular layer consisting mostly of glycoproteins (Hamazaki et al., '85; Begovac and Wallace, '86), was removed. The dechorionated zebrafish embryo is composed of two complex cellular compartments: a large yolk and the developing blastoderm (Fig. 1A). The major component of the yolk is vitellogenin, a large phospholipid (ca. 400 kDa; Mommson and Walsh, '88), stored in membrane-bound vesicles within the yolk. During early development in the zebrafish, the blastoderm progressively covers the yolk in a process known as epiboly (Westerfield, '93). After 100% epiboly, muscle segmentation begins, and these stages often are identified by the number of muscle somites present. Approximately three somites develop per hour (Westerfield '93). At the 128-cell stage, epiboly begins as the blastoderm envelopes the yolk, and ceases once the yolk is completely surrounded by blastoderm, i.e., 100% epiboly (Westerfield, '93). Underlying the blastoderm and covering the yolk is the yolk syncytial layer (YSL). This is a multinucleated layer (ca. 10-μm-thick) of nonyolky cytoplasm that begins to develop at approximately the 1,000-cell-stage in the zebrafish embryo (Kimmel and Law, '85). As the YSL develops, it replaces the thin (ca. 2-μm-thick), non-nucleated yolk cytoplasmic layer (Betchaku and Trinkhaus, '78). The YSL begins to envelop th yolk ahead of the blastoderm, and it surrounds the embryo by 100% epiboly (Solnica-Krezel and Driever, '94).

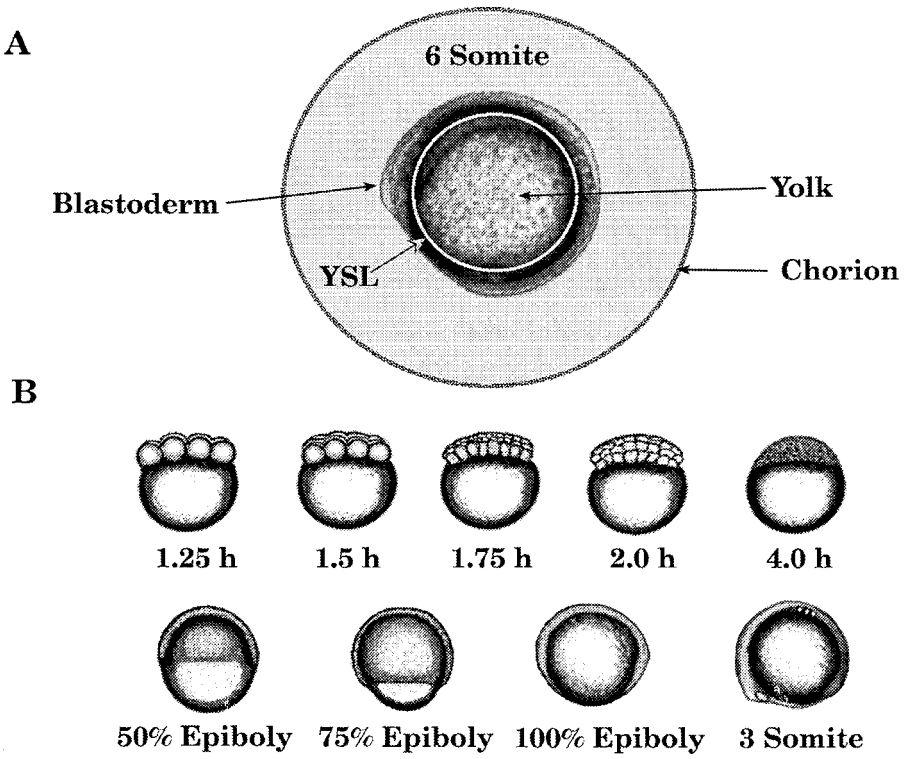

Fig. 1. **A**: Image of a 6-somite zebrafish embryo identifying the major compartments (yolk and blastoderm). Although the yolk syncytial layer (YSL) normally would not be visible in such an image, its position is included for clarity. Additionally, the position of the chorion is indicated, although this layer usually is removed in most preparations. **B:** Drawings depicting most of the developmental stages (described in hours from fertilization, by percent epiboly or by number of muscle somites present) used in these studies (modified from Westerfield, '93).

The complexity of the multicompartmental zebrafish embryo and the high amount of lipid present within the yolk challenged traditional cryobiological techniques. The objective of this study was to examine and describe the distribution and permeability behavior of water in dechorionated zebrafish embryos. We determined the hydraulic conductivity (L_p; Dick, '66, Leibo, '80) using osmotic volume change measurements. We used a variety of methods, including wet/dry measurements, electron spin resonance (ESR), magnetic resonance (MR) microscopy and Boyle van't Hoff measurements to determine the distribution of water in the zebrafish embryo. Throughout the study, only developmental time points up to the 6-somite stage were examined for two reasons. First, after each muscle somite forms, it develops an epithelial covering which could potentially act as a permeability barrier within the embryo (Westerfield, '93). Second, embryos still were relatively round, maintained a reproducible orientation when moved from solution to solution, and were nonmotile, simplifying the optical volumetric measurements.

Due to the complex nature of the zebrafish embryo, however, new techniques were needed to measure its water distribution. ESR has been used to quantitate the water volume of various cell types (Hammerstedt et al., '78; Kleinhans et al., '92). This usually requires the presence of a water-soluble spin label in the aqueous compartments of the cell and quenching of the extracellular signal with a broadening agent (Keith and Snipes, '74). However, zebrafish embryos are multicompartmental, and recent observations from our laboratory (Hagedorn et al., '96) indicate that a relatively impermeable barrier surrounds the yolk. Therefore, we used MR microscopy to assess the differences in the ability of the spin label to permeate into the two compartments of the embryo. A one-compartment model was used to determine the phenomenological water permeability characteristics of the cells in the embryo.

METHODS

Maintenance of animals

Animals were maintained according to Westerfield ('93). Briefly, 12 to 16 fish were kept in five liter aquaria (temp = 28.5°C; pH = 7.0) illuminated with a 12/12 light/dark cycle and fed dry flakes (Aquarian Diet, Mardel, Glendale, IL) and black worms (Tubifecidae). The developmental temperature was 28.5°C, and all developmental stages were described as in Westerfield ('93). All solutions throughout the study were prepared using embryo culture medium (EM; Westerfield, '93) which is a modified Hanks buffer. Figure 1B demonstrates the stages of development used in this paper.

Total water content of zebrafish embryos

We calculated the intracellular water content of 3- to 6-somite stage embryos (ca. 12 to 14 h) using wet/dry-weight and ESR measurements supported by MR microscopy.

In preliminary experiments, dechorionated embryos ruptured when the surrounding water was removed before weighing. Therefore, we toughened the surface of the embryos by cross-linking proteins with mild fixation (3% gluteraldehyde for 18 min). Gluteraldehyde was chosen because it yielded the best preservation of lipids and proteins for electron microscopy at this developmental stage (Hagedorn, unpublished data). We determined a minimum fixation time that allowed gentle mechanical contact with the surface of the embryos without hardening the entire tissue. Cellular dehydration of the embryos (n = 16) due to the hypertonic gluteraldehyde solution was assessed by measuring volume changes. Then, the embryos were distributed onto preweighed 22 x 22 mm glass coverslips (n = 70 to 100 embryos/coverslip), and the excess water was gently blotted away from each group of embryos. The coverslip with embryos was weighed on a balance (Sartorius Analytical A 120 S, accuracy tested to ±0.1 mg) and gently dried in an oven (50°C) for 2 to 5 days, then reweighed. The average of the wet weight and dry weight samples (n = 6) was determined.

To estimate the percentage of water in the yolk in 3-somite embryos, we punctured the yolk with a glass micropipette attached to a 1-ml syringe, and extracted yolk material by means of negative pressure with the syringe. The embryos were imaged under a stereomicroscope (Wild M5A at 500x) to ensure that the pipette tip (30–40 μm) was maintained within the center of the yolk, and thus only removing yolk material. Samples (n = 14) consisted of yolk from 1 or 2 embryos. Positive pressure was placed on the pipette to prevent uptake of embryo medium when moving from one yolk to another. Pipette contents (ranging in weight from 21–82 μg) were extruded onto preweighed 22 × 22 mm glass coverslips, weighed with a microbalance (Mettler MT5; accuracy ±0.8 μg), dried in an oven (50°C) for at least 8 hours and then reweighed.

Throughout this paper, results are presented as volume/volume (V/V) percents or fractions. To convert from weight/weight (W/W) measurements to V/V measurements, the following formula was used:

$$(V/V) = \rho_e \rho_w (W/W),$$

where p_e and p_w are embryo and water densities, respectively. Embryonic density was estimated from our observation that 3-somite embryos were neutrally buoyant in a 0.75-M sucrose solution (before any osmotic shrinkage occurred), yielding $\rho_e = 1.1$ g/cm^3. We defined neutral buoyancy as the concentration of sucrose at which the embryos remained suspended in solution (neither sinking to the bottom nor floating at the surface) before any osmotic shrinkage occurred.

ESR measurements of the aqueous spin label, tempone (4-oxo-2,2,6,6 tetramethylpiperidine-1-oxly, Molecular Probes, Eugene, OR) permit quantitative assessment of the water volume within cells (Hammerstedt et al., '78; Kleinhans et al., '92). MR imaging studies (Hagedorn et al., '96) suggested that little propylene glycol (PG) permeated the yolk. We used these same techniques to determine if the spin label could permeate the yolk. For ESR and MR experiments, we used tempone and the broadening agent chromium oxalate ($K_3[Cr(C_2O_4)_3] \cdot 3H_2O$; CrOx) synthesized according to the procedure of Bailar and Jones ('39). Tempone permeation into the yolk was inferred by measuring the change in water $1/T_2$ relaxation rate using MR microscopy. Because of tempone's relaxation properties (Koutcher et al., '84), its presence in the yolk would increase the $1/T_2$ relaxation rate (i.e., shorten the T_2 relaxation time) for water in this compartment. Embryos were immersed in 250 mM tempone solution for at least 60 min. MR images were collected following the methods of Hagedorn et al. ('95, '96), and T_2 measurements were made of the yolk and surrounding solution.

The volume of tempone-accessible intracellular water in zebrafish embryos was measured using ESR. Embryos (3 to 6 somites ca. 12 to 14 h; n = 150) were placed into an agar-coated, 35-mm Petri dish containing 4 ml of a solution (1,840 μl embryo medium + 160 μl of 50 mM tempone + 2,000 μl of 18.2 mM CrOx). Embryos were allowed to equilibrate for 20 min, and then were aspirated into a 100-μl glass capillary. Typically, after the embryos were loaded into the capillary, they were allowed to settle briefly (ca. 3 min), then placed in a Bruker ER200 X-Band spectrometer (Bruker Instruments, Billerica, MA) and measured repeatedly for 15 min. The spectrometer operated in a standard first derivative absorption mode, and its settings were: 3.5 mW power, ca. 20,000 gain, and 30 gauss sweep in 50 sec using a 50-msec detector time constant. A variation of our previous method (Kleinhans et al., '92) was used to determine the fraction of tempone-accessible water in the zebrafish embryos (see Appendix for details). Briefly, the strength of the intracellular (unbroadened) tempone and the extracellular (broadened) tempone signals were compared with standards to determine the tempone-accessible, intracellular and extracellular water. The remaining sample fraction was attributed to cell solids and tempone-inaccessible water. During measurements, allowance was made both for the sample settling (3 to 5 min) and reduction of the spin label (mean $\tau = 21$ min). The osmolality of all solutions was measured with a freezing-point depression osmometer (Advanced DigiMatic 3D2, Norwood, MA).

Osmotically inactive fraction (V_b)

Boyle van't Hoff experiments for determining V_b proved difficult to execute as discussed later. Ultimately, it only proved possible to measure V_b of the yolk using a nonpermeating solute, PG (Hagedorn et al., '96). Embryos at 100% epiboly (n = 22) were placed into 1.0-M PG and transferred stepwise into a 3.0-M PG solution (1.0, 2.0 M PG, 20 min each step). The 100% epiboly stage was chosen for these experiments because the embryos were spherical at this stage and maintained this shape throughout most of the long dehydration (>100 min). The blastoderm of later stages (i.e., 3- or 6-somite embryos) is less spherical and tended to warp during the long dehydration process, thus making the volume measurements inaccurate. Individual embryo images were digitized every 30 min over a 240-min period (3.0 M PG). The mean equilibrium yolk volume in 3-M PG and isotonic EM was plotted versus 1/osmolality, yielding the osmotically inactive volume of the yolk, or V_b.

Water permeability (L_p)

L_p was examined under two conditions, at the 4-hr or dome stage and at later developmental stages, as the blastoderm envelops the yolk. To do this, we measured the change in embryo volume in nonpermeating, hypertonic solutions. Changes in embryo size were measured during development (from 40% epiboly to 6-somite stage) using computer-assisted light microscopy. Embryos were examined under a Zeiss compound

microscope with a CCD camera (WV-BL200, Panasonic), images were digitized with a video frame-grabber card (LG3, Scion Corp., Frederick, MD), and stored for later morphometric analysis. Digitized images (100x) were displayed on a high resolution video monitor, and analyzed using a computer-aided morphometry package (Image 1.45, NIH, Bethesda, MD). The outline of each embryo was determined by the computer, or parts of the embryo were outlined manually (with the mouse), and linear, planar, and volumetric parameters of each embryo were calculated. The major and minor axes were used to determine the volume of embryos at all stages using a prolate spheroid formula ($V = 4/3\pi\ ab^2$), where a and b were the major and minor semi-axes, respectively.

Embryos (dome stage to 6-somite) were placed in 0.35 M NaCl and 0.6% agarose (SeaPrep, FMC Corp., Rockland, ME), for 25 to 31 min, and images digitized every 2 min. At the dome stage, the blastoderm perches atop the yolk leaving much of the yolk freely visible. For the dome stage embryos, only the yolk volume was measured using image analysis, whereas at later developmental stages, the entire embryo volume was measured.

The water permeability (L_p) of the yolk and the entire embryo was determined using a simple phenomenological model in which both the embryo and yolk were modeled as a single compartment (lumped parameter model; Leibo, '80; Lin et al., '89). Our objective in modeling the permeability characteristics of the zebrafish embryo was to develop a simple phenomenological model that fit the data and allowed predictions of the volumetric response of embryos during cryopreservation treatments. The rate of cell volume change resulting from a water efflux or influx is given by:

$$dV_w/dt = L_pART(M^i - M^e) \quad (1)$$

where V_w is the cell water volume, A the compartment area (assumed to be constant), L_p the water permeability, R the gas constant, T the absolute temperature, and M^i and M^e (the intracellular and extracellular solution osmolalities, respectively, Dick, '66). When no permeating solute is present, as is the case here, only water crosses the membrane and $dV_w/dt = dV_c/dt$ where V_c is the microscopically observed total cell volume. Thus

$$dV_c/dt = L_pART(M^i - M^e) \quad (2)$$

The external osmolality M^e was fixed by the test conditions (M^e = 0.683 osmolal consisting of 0.35 M NaCl, 40 mosm embryo medium and 0.6% agarose). The internal osmolality was computed assuming a linear Boyle van't Hoff relationship:

$$M^i = M^I_o(1 - V_b)V_o/V_w \quad (3)$$

where M^i_o was assumed to have an isosmotic value of either 0.04 or 0.30 osmolal, V_o was the isosmotic total cell volume and V_b was the osmotically inactive cell volume fraction (under isosmotic conditions). Equation 2 was numerically integrated using an adaptive Runge-Kutta method and least squares fit to the microscopically measured V_c data using a modified Powell algorithm as implemented in the program Scientist (Micromath, Salt Lake City, UT). The parameters determined (fitted) were L_p and V_o. The osmotically inactive volume fraction (V_b) was either fitted or independently determined (see Discussion). The isotonic value for zebrafish embryos is unknown. After dechorionation, embryos were raised in 40 mosm EM. However, most animal cells have an internal osmotic strength of ca. 300 mosm (Guyton, '81). We used both values as isotonic in these modeling studies.

Analysis

Throughout this paper, data pairs presented as percentages were statistically tested for equality by a Chi-square analysis or a Mann Whitney U-test (Sokal and Rolf, 1969).

RESULTS

Total water content of zebrafish embryos

Accurately measuring wet/dry weight was difficult, because dechorionated embryos were extremely fragile, but light fixation circumvented this problem. Three somite embryos had a mean water content of 73.6 ± 1% S.E.M. (n = 3; samples of 70 to 90 embryos/sample), and fixation did not cause any volumetric change before drying ($P > 0.05$). Wet/dry measurements of the extracted yolk yielded a water content of 41.7 ± 1% (n = 14). Unfortunately, making accurate wet/dry measurements for the aggregate of cells in the blastoderm was not possible. To determine the percentage of water within the blastoderm, we used ESR in conjunction with MR microscopy. MR images revealed that tempone caused a fivefold increase in the $1/T_2$ relaxation rate of the signal from the medium surrounding the embryos (tempone = 47.8 ± 3.5 1/sec; n = 3; controls = 8.6 ± 1.7 1/sec; n = 3), and only a 9% increase in the $1/T_2$ rate within the yolk (control values from Hagedorn et

al., '95, '96). After at least 60 min of equilibration in tempone, the $1/T_2$ rate within the yolk remained at control values (tempone = 97.7 ± 3.1 1/sec; n = 2; controls = 89.6 ± 7.3 1/sec; n = 3; $P > 0.05$). This suggested that tempone failed to permeate the yolk, and that ESR was only capable of detecting water within the blastoderm. Utilizing ESR, the water within the 3- to 6-somite embryo was measured, yielding 32 ± 5 % (tempone-accessible water volume/total embryo volume). Assuming that the blastoderm constituted 39% (V/V) of the 6-somite embryo, yields an ESR determined blastoderm water volume of 82 ± 13 S.E.M. % (determined by 32% blastoderm water volume/39% total blastoderm volume). Because the distribution of water and solids in the embryo changes throughout development as the blastoderm grows, the 6-somite stage was chosen to describe this distribution (Fig. 2).

Osmotically inactive fraction of water (V_b)

Measuring the osmotically inactive fraction (V_b) of the embryo proved difficult using Boyle van't Hoff techniques. Because of the low water permeability of the zebrafish embryo, equilibration times were long (hours, during which the embryo continues to develop). To compensate for this, very high nonpermeating solute concentrations were used which introduced new problems including cell rupture in NaCl and embryo buoyancy in sucrose. Only PG proved satisfactory, and although the blastoderm was permeable to PG, the yolk was impermeable to PG (Hagedorn et al., '96). Therefore, using Boyle van't Hoff techniques, we analyzed the volume of the yolk compartment alone, rather than the entire embryo. At approximately 180 min after dehydration onset, the yolk (of 100% epiboly embryos) equilibrated in the 3.0-M PG solution (1/osm = 0.254). Using this equilibrated volume and those in 40-mosm EM, a Boyle van't Hoff plot was constructed, yielding a V_b of 0.78 for the yolk compartment. It was also possible to determine V_b from the kinetic data, yielding V_b values from 0.41 to 0.66 (as discussed in detail in the next section).

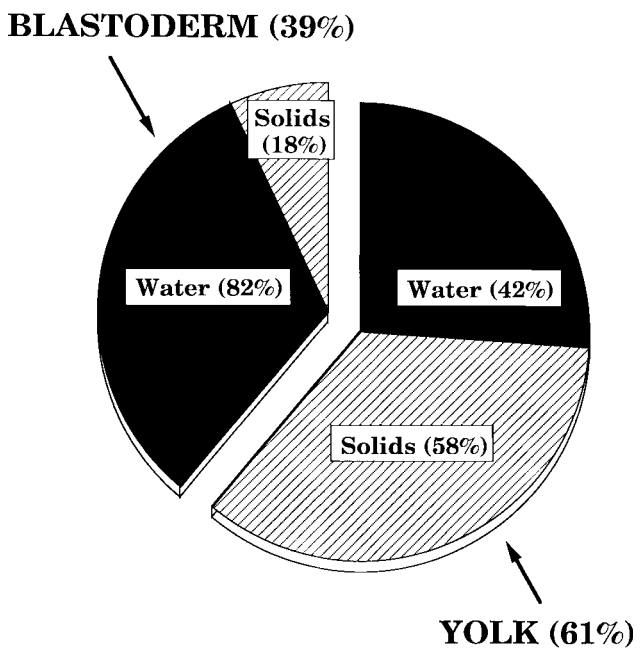

Fig. 2. Water is unequally distributed in the compartments of the zebrafish embryo. Also, the distribution of these constituents changes throughout development as the blastoderm grows. In this example, the distribution of the water and solids in the blastoderm and yolk of a 6-somite embryos is shown.

Water permeability (L_p)

The L_p characterizes the rate at which water moves into or out of the entire embryo. To determine if water permeability changed during development, we examined the dehydration patterns at four developmental stages (75% epiboly to 6-somite stages) in a 0.35-M NaCl solution (plus 40 mosm EM and 0.6% agarose; Fig. 3). Exosmosis occurred slowly with equilibrium not being reached during the 31-min time course of the experiment. However, the L_p could be determined for each of these developmental stages by fitting the experimental data to a simple one-compartment model. The L_p depends on the assumed intracellular, isosmotic osmolality (M^i_o) and is reported below for both an M^i_o of 40 and 300 mosm. Figure 4 illustrated typical model fits to the data with L_p and V_o as fitting parameters (V_b of the entire embryo was set at 0.55, see Discussion for details). The mean L_p changed ($P < 0.05$) during development. During the 75% epiboly to 3-somite stage, L_p remained constant, then increased at the 6-somite stage (see Table 1). The mean L_p (± S.E.M.) for the two groups was 0.022 ± 0.002 and 0.049 ± 0.008 μm x $min^{-1}atm^{-1}$ assuming M^i_o = 40 mosm or 0.040 ± 0.004 and 0.100 ± 0.017 μm × min^{-1} atm^{-1} assuming M^i_o = 300 mosm. We also measured the L_p of the yolk (n = 8) at the dome stage where ca. 80% to 90% of the yolk was directly exposed to a nonpermeating salt solution (Fig. 5). Using the same one-compartment model yielded a mean L_p (± S.E.M.) for the yolk of 0.144 ± 0.033 (M^i_o = 40 mosm) or 0.35 ± 0.11 μm x $min^{-1}atm^{-1}$ (M^i_o = 300 mosm). These mean values of L_p for the yolk were ca. five to eight times those measured for the entire embryo. In a few preliminary

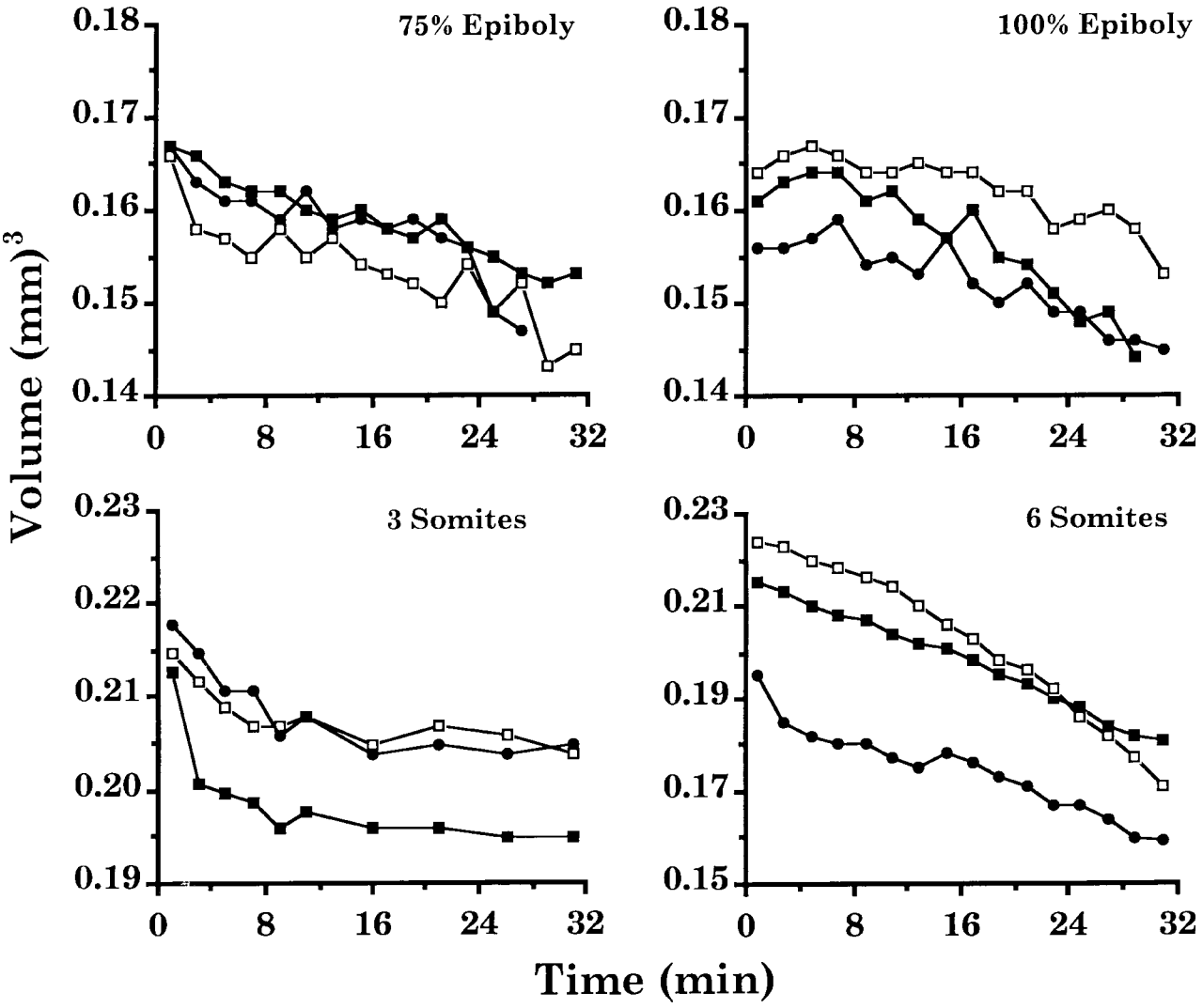

Fig. 3. Dehydration pattern of zebrafish embryos at different developmental stages (75% epiboly to three somites; n = 3 for each graph) immersed in a solution of 0.35 M NaCl in 40 mosm embryo culture medium (EM) and 0.6% agarose at t = 0. Exosmosis occurred slowly with no evident equilibration during the observation period.

experiments, L_p of the yolk was reduced by one to two orders of magnitude by the presence of 3 M propylene glycol in the external medium (data not shown). In addition to L_p, it was possible to fit V_b using the yolk kinetic data, yielding a value of V_b(yolk) = 0.66 ± 0.07 (M^i_o = 40 mosm) or 0.41 ± 0.05 (M^i_o = 300 mosm) which is appreciably less than the V_b(yolk) of 0.78 obtained in the Boyle van't Hoff experiments.

DISCUSSION

Our objective in these studies was to examine the distribution of water and cellular permeability characteristics of teleost embryos because a key to successful cryopreservation lies in understanding these complex phenomena (Mazur, '70, '84).

Measuring the relative proportion of water and solids in the various zebrafish embryo compartments is essential for eventually achieving successful cryopreservation. Our data revealed that the intracellular water was unequally distributed between the yolk and blastoderm compartments. The total percentage of water in the 6-somite zebrafish embryo and yolk (as determined by dry weight and ESR measurements) was similar to values reported for other species of fish and for birds (Table 2).

Comparison of the water content of the individual embryo compartments with the total em-

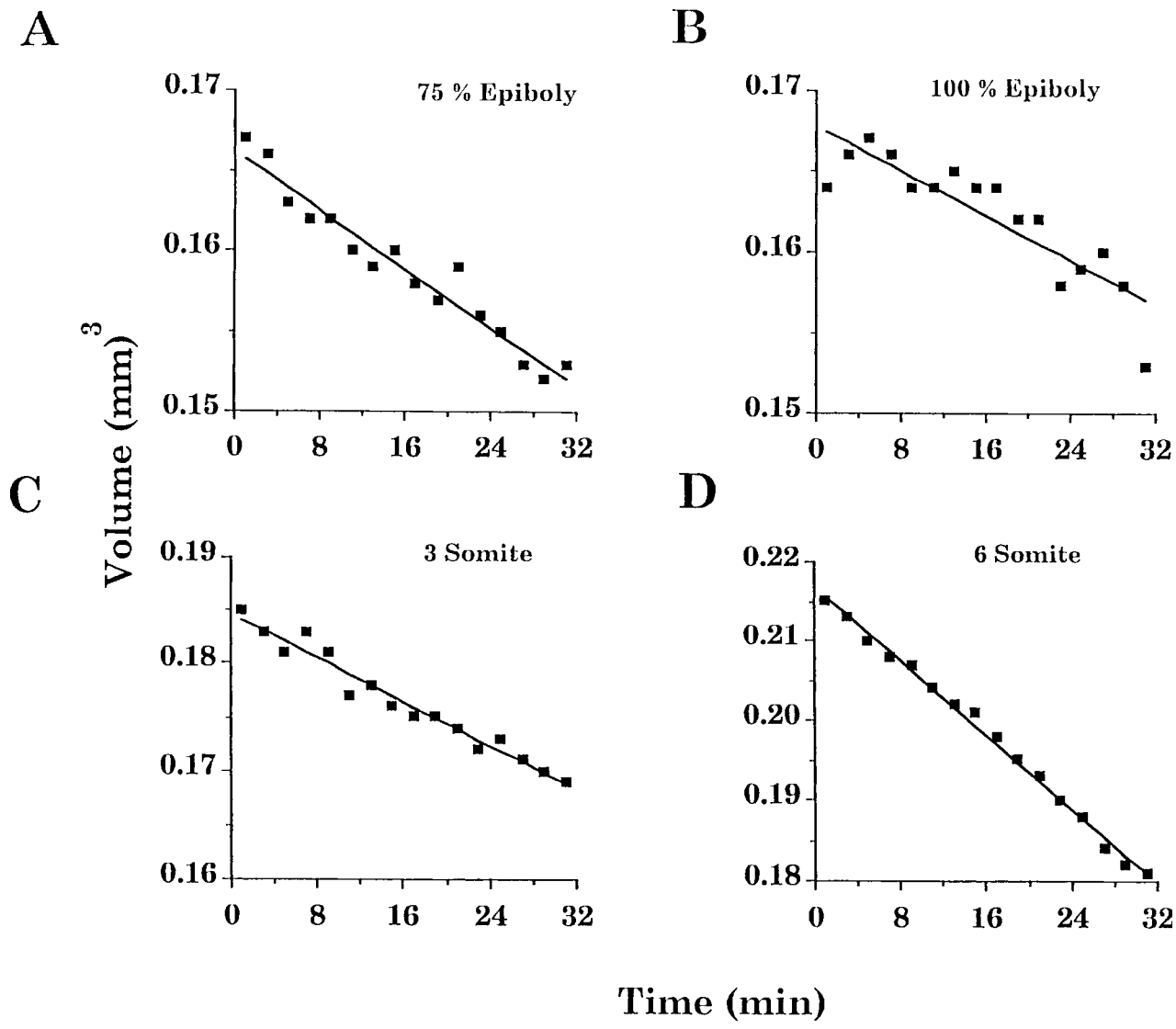

Fig. 4. **A–D:** Examples from Figure 3 of volume versus time relationships (symbols). Embryos at various developmental stages (75% epiboly to the 6-somite) were modeled as a single compartment. The solid curves show a least-squares fit for a water-permeability model, assuming an intracellular isosmolality of 40 mosm. In these examples, the embryo volumes did not approach equilibrium during the osbervation period, so V_b was fixed at 0.55 and L_p and V_o were fit to the data. See Table 1 for specific L_p values.

bryo water content showed some discrepancies. At the 6-somite stage, the yolk contained ca. 61% of the total volume and 42% water, whereas the blastoderm contained 39% of the total volume and 82% water. This yielded a total embryo water content of 58% (0.61 x 0.42 + 0.39 × 0.82 = 0.58); however, dry weight measurements of the embryos indicated a total water content of 74%. Most likely, these dry weight measurements overestimated the water content, due to the excess unremovable water adher-

TABLE 1. Phenomenological L_p data for zebrafish embryos

	Mean L_p (±S.E.M.) μm × $min^{-1}atm^{-1}$				
Isotonic value (mosm)	75% epiboly	100% epiboly	3-somiate	6-somite	*P*
40	0.022 ± 0.001	0.022 ± 0.005	0.022 ± 0.003	0.049 ± 0.008	<0.05
300	0.041 ± 0.002	0.041 ± 0.011	0.040 ± 0.005	0.100 ± 0.017	<0.05
n	3	3	9	3	

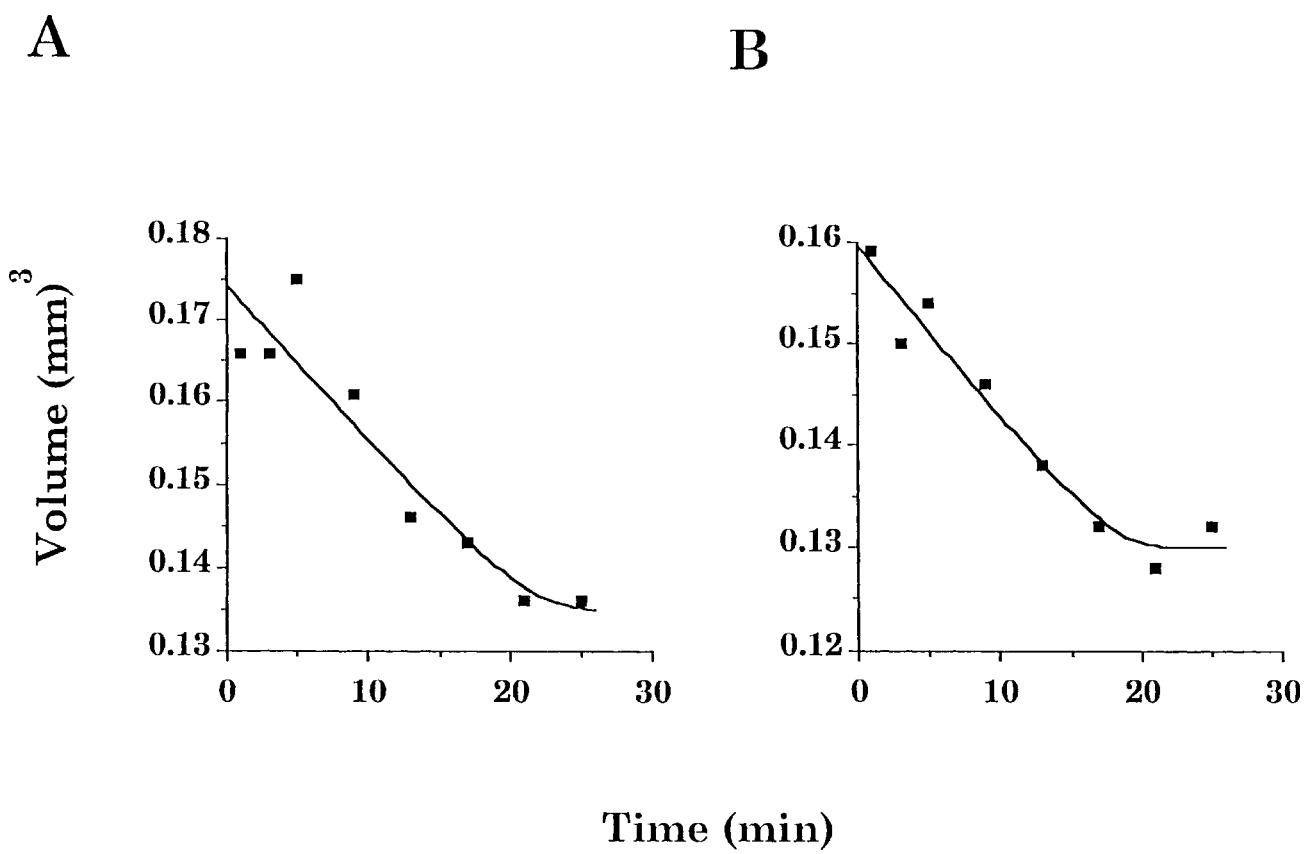

Fig. 5. Examples of volume versus time relationships (symbols) for the yolk of dome-stage embryos immersed in a nonpermeating solute (0.35 M NaCl in 40 mosm EM and 0.6% agarose) at t = 0 were modeled as a single compartment. The solid curves show a least squares fit for a water-permeability model assuming 40 mosm intracellular isosmolality.

ing to the outer surfaces of the embryos before weighing. Additionally, the percentage volumes of the blastoderm and yolk were based upon planar measurements. Since the 6-somite embryo shows a great deal more structure than earlier round stages, these planar measurements may have underestimated the percent volume of the blastoderm.

The isosmotic value of the zebrafish embryo cytoplasm is unknown. However, after dechorionation, zebrafish embryos that were cultured in 40 mosm embryo medium did not undergo an increase in volume. The isosmotic value of most animal cells is ca. 300 mosm (Guyton, '81). If this is the case for zebrafish embryos, then after being placed in 40 mosm medium, embryo cells would experience ca. 7 atmospheres of pressure as a result of the osmotic gradient. Electron microscopic analysis (Hagedorn, unpublished data) revealed that no physical structures existed within the dechorionated embryos that could withstand this amount of pressure. Another possible explanation for this lack of osmotic response in a hypotonic

TABLE 2. Contents of egg or embryos of some yolk-laden species

	Total (%)		Yolk (%)		
	Water	Solids	Water	Solids	References
Fish					
Coho salmon eggs	61.0	39.0	—	—	Hardy et al. ('84)
Rainbow trout eggs	66.2	33.8	—	—	Blaxter ('69)
Sardine eggs	70.7	29.3	—	—	Blaxter ('69)
6-somite zebrafish embryo	74.0	26.0	42	58	This study
Birds					
Chicken egg	73.6	26.4	48.7	51.3	Romanoff and Romanoff ('49)

environment is active water pumping. This would remove the water as rapidly as it entered. Long-term cold storage should inactivate these pumps and produce swelling. This has never been observed in 100% epiboly to 3-somite zebrafish embryos stored at 4°C for 10–16 hours (Hagedorn, unpublished observation). How does the zebrafish embryo maintain a normal cell volume in a supposedly hypotonic medium? One possible explanation may be the sequestration and binding of ions in vacuoles or organelles within their cells, thereby reducing the functional osmolality of cytoplasm. Ion sequestration is a relatively common physiological mechanism found in unicellular organisms, such as halobacteria, that must adapt to a variety of osmotic environments (reviewed in Harris, '72).

Our experimental data concerning the osmotic loss of cellular water are adequately described by a simple one-compartment model with little or no change in L_p during development. This phenomenological L_p reflects an overall response of the embryo and should not be treated as the permeability of individual cells or membranes. Further, our determination of L_p makes the conventional assumption that the cell compartment(s) follow linear Boyle van't Hoff behavior (Eq. 3) as frequently observed (Dick, '66; Leibo, '80; Lin et al., '89; Le Gal et al., '94). It was not possible, experimentally, to test this assumption of linearity in our Boyle van't Hoff experiments because of the difficulties previously discussed. In general, linear behavior is a reasonable assumption for cells without a cell wall which are, therefore, unable to sustain any appreciable membrane tension. However, as noted, these embryos may exhibit some form of osmoregulatory behavior. Osmoregulation works to minimize volume excursions away from isosmotic and consequently would lead to an underestimate of the true L_p. We cannot preclude this possibility. Substantially more work will be required to clarify this issue of osmoregulation. However, even if osmoregulation is present, it can be argued that our (phenomenological) L_p values reflect the actual rate at which water can be removed from the embryo compartments and, therefore, are cryobiologically relevant. Conversely, extrapolation of these results to subzero temperatures is more problematic if osmoregulation is present. Our limited Boyle van't Hoff data also make an accurate determination of V_b for the yolk compartment difficult. However, as noted below, L_p is insensitive to the value of V_b chosen and thus is not a major concern.

In general, the kinetic volume response curves are composed of an initial dynamic portion (reflecting the system's response to the altered osmotic environment) followed by a constant portion (achieved upon equilibrium). The dynamic portion shape is principally determined by L_p, whereas the constant portion depends primarily on V_b. When both portions of the curve are present, both L_p and V_b can be calculated, as in Figure 5. However, when the constant portion is missing (as in Fig. 4, and to some degree in Fig. 5), the experimental data do not constrain V_b, and a value must be chosen before fitting the remaining parameters. For values of V_b (embryo) between 0.3 and 0.8, the fitted value of L_p varied by less than 4% for each data set at each developmental stage. To estimate V_b(embryo) at the 6-somite stage, we made the following assumptions: the yolk comprised 61% of the volume and has V_b(yolk) = 0.78 (based on the Boyle van't Hoff data); the blastoderm comprised 39% of the volume and has an assumed V_b(blastoderm) = 0.20 (estimated from typical values in Dick, '66; Leibo, '80; Le gal et al., '94). Therefore, the V_b(embryo) = 0.55 as determined by V_b(yolk) × yolk fractional volume + V_b(blastoderm) × blastoderm fractional volume. This value was used to determine L_p of the entire embryo.

The estimated mean water permeabilities for the zebrafish embryo (0.022 to 0.100 $\mu m \times min^{-1}atm^{-1}$, depending on the isosmotic value used) were considerably less than those of other embryos, such as *Drosophila* (0.722 $\mu m \times min^{-1}atm^{-1}$; Lin et al., '89) and mice (0.43 $\mu m \times min^{-1}atm^{-1}$; Leibo, '80). These later values were also determined using a one-compartment model. The low permeability of the zebrafish embyro, coupled with its large size (and consequent low area to volume ratio), lead to a very slow osmotic response. In the preliminary experiments, the presence of propylene glycol reduced L_p even further. If this proves to be a general effect of cryoprotectants on Zebrafish embryos, it makes the removal of intracellular water during cryopreservation even more difficult. The reduction of L_p in the presence of cryoprotectants has been observed in many cases, eg. human sperm (Gilmore et al., '95) and human RBC (Toon and Solomon, '90).

L_p changed during development. At the 75% to 3-somite state, L_p of the embryo was 0.022 to 0.040 $\mu m \times min^{-1}atm^{-1}$, whereas at the 6-somite stage the L_p was 0.049 to 0.100 $\mu m \times min^{-1}atm^{-1}$. The twofold increase in L_p at the 6-somite may be an artifact of the increasing morphological complexity of the embryo volume. At this stage, the volume may not be well approximated by a prolate sphere. Three-dimensional vol-

ume reconstruction using confocal microscopy may resolve how well planar measurements approximate the changing volume of the developing zebrafish embryo. Additionally, although there are no other comparable water permeability data for other fish embryos, Harvey and Chamberlain ('82) used deuterated water exchange to try to identify the developmental stages with the highest water permeability. Unfortunately, these data can be difficult to compare because, if water channels are present, the diffusional permeability (P_d) from water exchange across the membrane may differ from the osmotic permeability (P_f) describing a water flux in the presence of an osmotic gradient.

Vertebrate and invertebrate embryos express a wide range of osmotically active volumes. Some vertebrate embryos (e.g., cattle, mice and cats) have a V_b from 0.15 to 0.32 ('80; Leibo et al., '74; Leibo, '77; Mazur and Schneider, '86; Wood et al., '91). In contrast, invertebrate embryos (e.g., clams and fruit flies) have higher V_b values of 0.47 and 0.54, respectively (Lin et al, '89, '93). On the basis of the previous discussion, we estimated that the V_b for the entire zebrafish embryo was 0.55, similar to those of other embryos with yolk, including the clam and fruit fly. Unfortunately, there are no other comparative V_b measurements for fish embryos.

Although teleost embryos present many challenges for cryopreservation, the water permeability and distribution data, presented here, are a first step in developing cryopreservation protocols for fish embryos. It is noteworthy that *Drosophila* embryos recently have been cryopreserved successfully by vitrification (Steponkus et al., '91; Mazur et al., '92). This achievement has guided our research strategy, because the relative size and complex composition (i.e., blastoderm and yolk compartments) of the *Drosophila* embryo are relatively similar to those of fish (Lin et al., '89; Rall, '93). An advantage of vitrification is that it allows rapid freezing rates using a simple, cost-effective approach with improved embryo survival (Rall and Fahy, '85; Rall, '92, '93). The cross-species applicability of this technique has been demonstrated by the successful vitrification of cattle (Massip et al., '86, '87), rabbit (Smorag et al., '89), sheep (Schiewe et al., '91) and fruit fly (*Drosophila*) (Steponkus et al., '91; Mazur et al., '92) embryos. Vitrification also shows great promise as a conservation tool because: (1) it is extremely rapid, so that a large number of germ plasm samples can be processed quickly; (2) it does not require sophisticated, computer-controlled equipment, but only liquid nitrogen that is transportable and available in most developing countries; and (3) most importantly, it may improve post-thaw viability of cryopreserved germ plasm.

ACKNOWLEDGMENTS

We thank Dr. Monte Westerfield and Dr. Ruth Bremiller, University of Oregon, Dr. John Critser of Methodist Hospital of Indiana Inc., and Dr. Olav Oftedal and Michael Jakubasz of the National Zoological Park for use of their laboratories, equipment and histological material during these experiments, the anonymous reviewer, and Dr. Peter Mazur at the Oak Ridge National Laboratory, Oak Ridge, TN for their discussion and comments on the manuscript. Dr. Lee-Ann Hayek of the Smithsonian Institution kindly provided statistical assistance. This work was supported by grants to MH from the National Institutes of Health (R29 RR08769), Friends of the National Zoo, Maryland Sea Grant College, the National Aquarium in Baltimore, and the Smithsonian Institution.

LITERATURE CITED

Bailar, J.C., and E.M. Jones (1939) Trioxalato salts. Inorg. Synthesis, *1*:35–38.

Ballou, J.D. (1992) Potential contribution of cryopreserved germ plasm to the preservation of genetic diversity and conservation of endangered species in captivity. Cryobiology, *29*:19–25.

Begovac, P.C., and R.C. Wallace (1986) Vitelline envelop proteins in the pipefish. J. Morphol., *193*:117–133.

Blaxter, J.H.S. (1953) Sperm storage and cross-fertilization of spring and autumn spawning herring. Nature (Lond.) *172*:1189–1190.

Blaxter, J.H.S. (1969) Development: Eggs and larvae. In: Fish Physiology Vol. III. W.S. Hoar and D.J. Randall, eds. Academic Press, New York, pp. 177–253.

Betchaku, T., and J.P. Trinkhaus (1978) Contact relations, surface activity, and cortical microfilaments of marginal cells of the enveloping layer and of the yolk syncytial and yolk cytoplasmic layers of *Fundulus* before and during epiboly. J. Exp. Zool. *206*:381–426.

Dick, D.A.T. (1966) Cell Water. Butterworths, London.

Gilmore, J.A., L.E. McGann, J. Liu, D.Y. Gao, A.T. Peter, F.W. Kleinhans, and J.K. Critser (1995). Effect of cryoprotectant studies on water permeability of human spermatozoa. Biol. Reprod. *53*:985–995.

Guyton, A.C. (1981) Textbook of Medical Physiology, 6th ed. W.B. Saunders, Philadelphia.

Hagedorn, M., E. Hsu, D.E. Wildt, W.F. Rall, and S.J. Blackband (1995) Progress on creating a genetic bank for endangered species of fish: II. Permeability studies of dechorionated zebrafish embryos. Cryobiology, *32*:567.

Hagedorn, M., E. Hsu, U. Pilatus, D.E. Wildt, W.F. Rall and S.J. Blackband (1996) Magnetic resonance microscopy and spectroscopy reveal kinetics of cryoprotectant permeation in a multicompartmental biological system. Proc. Nat. Acad. Sci., *93*:7454–7459.

Hamazaki, T., I. Iuchi, and K. Yamagami (1985) A spawning female-specific substance reactive to anti-chorion (egg enve-

lope) glycoprotein antibody in the teleost, *Oryzias latipes*. J. Exp. Zool., *235*:269–279.

Hammerstedt, R.H., A.D. Keith, W. Snipes, R.P. Amann, D. Arruda, and L.C. Greil (1978) Use of spin labels to evaluate effects of cold shock and osmolality on sperm. Biol. Reprod. *18*:686–696.

Hardy, R.W., K.D. Shearer, and I.B. King (1984) Proximate and elemental composition of developing eggs and maternal soma of penreared Coho Salmon (*Oncorhynchas kisutch*) fed production and trace element fortified diets. Aquaculture, *43*:147–165.

Harris, E.J. (1972) Transport and Accumulation in Biological Systems. Butterworths, London, pp. 1–454.

Harvey, B., and J.B. Chamberlain (1982) Water permeability in the developing embryo of the zebrafish, *Brachydanio rerio*. Can. J. Zool., *60*:268–270.

Harvey, B., R.N. Kelley, and M.J. Ashwood-Smith (1983) Permeability of intact and dechorionated Zebrafish (*Brachydanio rerio*) embryos to glycerol and dimethyl sulfoxide. Cryobiology *20*:432–439.

Hisaoka, K.K., and H.I. Battle (1958) The normal developmental stages of the zebrafish, *Brachydanio rerio* (Hamilton-Buchanan) J. Morphol., *102*:311–328.

Hisaoka, K.K., and C.F. Firllit (1960) Further studies on the embryonic development of the zebrafish, *Brachydanio rerio* (Hamilton-Buchanan) J. Morphol., *107*:205–255.

Keith, A.D., and W. Snipes (1974) Viscosity of cellular protoplasm. Science, *183*:666–668.

Kimmel, C.B., and R.D. Law (1985) Cell lineage of zebrafish blastomeres. II. Formation of the yolk syncytial layer. Dev. Biol., *108*:86–93.

Kleinhans, F.W., V.S. Travis, J. Du, P.M. Villines, K.E. Colvin, and J.K. Critser (1992) Measurement of human sperm intracellular water volume by electron spin resonance. J. Androl., *13*:498–506.

Koutcher, J.A., C.T. Burt, R.B. Lauffer, and T.J. Brady (1984) Contrast agents and spectroscopic probes in NMR. J. Nucl. Med., *25*:506–513.

Le Gal, F., P. Gasqui, and J.P. Renard (1994) Differential osmotic behavior of mammalian oocytes before and after maturation: A quantitative analysis using goat oocytes as a model. Cryobiology, *31*:154–170.

Leibo, S.P. (1977) Fundamental cryobiology of mouse ova and embryos. In: The Freezing of Mammalian Embryos. K. Elliot and J. Whelan, eds. Elsevier, Amsterdam, pp. 69–92.

Leibo, S.P. (1980) Water permeability and its activation energy of fertilized and unfertilized mouse ova. J. Memb. Biol. *53*:179–188.

Leibo, S.P., P. Mazur, and S.L. Jackowski (1974) Factors affecting survival of mouse embryos during freezing and thawing. Exp. Cell Res., *89*:79–88.

Lin, T.-T., R.E. Pitt, and P.L. Steponkus (1989) Osmotic behavior of *Drosophila melanogaster* embryos. Cryobiology, *26*:453–471.

Lin, T.-T., H-T. Tung, and N-H. Chao (1993) Osmometric characteristics of hard clam eggs. Cryobiology, *30*:19.

Massip, A., P. van der Zwalmen, B. Scheffen, and F. Ectors (1986) Pregnancies following transfer of cattle embryos preserved by vitrification. Cryo-Letters, *7*:270–273.

Massip, A. P. van der Zwalmen, and F. Ectors (1987) Recent progress in cryopreservation of cattle embryos. Theriogenology, *27*:69–79.

Mazur, P. (1970) Cryobiology: The freezing of biological systems. Science, *168*:939–949.

Mazur, P. (1984) Freezing of living cells: Mechanisms and implications. Am. J. Physiol., *247*:C125–C142.

Mazur, P., and U. Schneider (1986) Osmotic responses of preimplantation mouse and bovine embryos and their cryobiological implications. Cell. Biophys., *8*:259–285.

Mazur, P., K.W. Cole, J.W. Hall, P.D. Schreuders, and J.W. Mahowald (1992) Cryobiological preservation of *Drosophila* Embryo. Science, *258*:1932–1935.

Mommson, T.P., and P.J. Walsh (1988) Vitellogenesis and oocyte assembly. In: Fish Physiology. Vol. XI, W.S. Hoar and D.J. Randall, eds. Academic Press, New York, pp. 348–407.

Rall, W.F. (1992) Cryopreservation of oocytes and embryos: Methods and applications. Anim. Reprod. Sci., *28*:237–245.

Rall, W.F. (1993) Recent advances in the cryopreservation of salmonid fishes. In: Genetic Conservation of Salmonid Fishes. J.G. Cloud and G.H. Thorgaard, eds. Plenum Publishing Corporation, New York, pp. 137–158.

Rall, W.F., and G.M.Fahy (1985) Ice-free cryopreservation of mouse embryos at –196°C by vitrification. Nature, *313*:573–575.

Romanoff, A.L., and A.J. Romanoff (1949) The Avian Egg. John Wiley & Sons, Inc, New York, pp. 1–918.

Schiewe, M.C., W.F. Rall, L.D. Stuart, and D.E. Wildt (1991) Analysis of cryoprotectant, cooling rate, and *in situ* dilution using conventional freezing of vitrification for cryopreserving sheep embryos. Theriogenology, *36*:279–293.

Smorag, Z., B. Gajda, B. Wieczorek, and J. Jura (1989) Stage-dependent viability of vitrified rabbit embryos. Theriogenology *31*:1227–1231.

Sokal, R.S., and F.J. Rohlf (1969) Biometry. W.F. Freeman and Company, San Francisco, pp. 1–776.

Solnica-Krezel, L., and W. Driever (1994) Microtuble arrays of zebrafish yolk cell: Organization and function during epiboly. Development *120*:2443–2455.

Steponkus, P.L., S.P. Myers, D.V. Lynch, R.E. Pitt, T-T. Lin, R.J. MacIntyre, S.P. Leibo, and W.F. Rall (1991) Cryobiology of *Drosophila melanogaster* embryos. In: Insects at Low Temperature. R.E. Lee and D.L. Denlinger, eds. Chapman and Hall, New York pp. 408–423.

Toon, M.R. and A.K. Solomon (1990) Transport parameters in the human red cell membrane: solute-membrane interactions of hydrophilic alcohols and their effect on permeation. BBA *1022*:57–71.

Westerfield, M. (1993) The Zebrafish Book. A Guide for the Laboratory Use of Zebrafish (*Brachydanio rerio*). University of Oregon Press, Eugene.

Wildt, D.E. (1992) Genetic resource banking for conserving wildlife species: Justification, examples and becoming organized on a global basis. Anim. Reprod. Sci., *28*:247–257.

Wildt, D.E., U.S. Seal, and W.F. Rall (1993) Genetic resource banks and reproductive technology for wildlife conservation. In: Genetic Conservation of Salmonid Fishes. J.G. Cloud and G.H. Thorgaard, eds., Plenum Publishing Corporation, New York, pp. 159–173.

Wood, T.C., D.E. Wildt, L.A. Johnston, A.M. Donoghue, and W.F. Rall (1991) Osmometric behavior of domestic cat embryos in solutions of sucrose and permeating cryoprotectants. Cryobiology *28*:572.

Zhang, T. and D.M. Rawson (1995) Studies on chilling sensitivity of zebrafish (*Brachydanio rerio*) embryos. Cryobiology, *32*:239–246.

Zhang, T., and D.M. Rawson (1996) Feasibility studies on vitrification of intact zebrafish (*Brachydanio rerio*) embryos. Cryobiology, *33*:1–13.

Zhang, T., D.M. Rawson, and G.J. Morris (1993) Cryopreservation of pre-hatch embryos of zebrafish (*Brachydanio rerio*) embryos. Aqua. Livi. Res., *6*:145–153.

Appendix: Measurement of Intracellular Water Volume in Multicompartmental Systems Such as the Zebrafish Embryo

F.W. KLEINHANS[1] AND M. HAGEDORN[2]
[1]*Department of Physics, Indiana University-Purdue University Indianapolis, Indianapolis, IN 46202*
[2]*Smithsonian Institution, National Zoological Park and Conservation and Research Center, Washington, DC 20008*

Measurement of the total volume available to dissolve a solute in biological systems is important for basic and applied studies in cryobiology, physiology, pharmacology, and other biomedical fields. Electron Spin Resonance (ESR) permits accurate measurements of intracellular water volume and has been applied to vesicles (Vistnes and Puskin, '81), mammalian sperm (Hammerstedt et al., '78; Kleinhans et al., '92), and red blood cells (Moronne et al., '90; Kleinhans at al., '92). The goal of this appendix is to show in greater detail the assumptions and modifications used in calculating the intracellular water volume of the zebrafish embryo using ESR.

In traditional methodologies, cells and the suspending medium are labeled with a water-soluble spin label (e.g., tempone) which freely permeates cells by rapidly diffusing and equilibrating across the cell membranes. The extracellular label signal is then broadened nearly to extinction using a broadening agent that is membrane-impermeable (e.g., chromium oxalate, CrOx). The remaining intracellular signal is compared with a standard prepared in an identical ESR sample tube containing only spin label and suspending medium. Then, for example, if the intracellular signal has one-quarter the intensity of the standard, we know that the aggregate intracellular water volume is one-quarter of the sample volume. Finally, if the concentration of cells in the sample is known, this result can be converted to an intracellular water volume per cell (Hammerstedt et al., '78).

Unfortunately, this approach cannot be applied directly to multicompartmental biological systems due to: (1) the difficulty of assessing the volume of individual compartments; (2) the possible presence of permeability barriers that prevent the permeation of the spin label; and (3) the inability of determining the cell concentration. With small cells, such as red blood cells, samples are prepared and divided, using one part for ESR and the other for cell concentration determination (i.e., with a hemocytometer). The 3- to 6-somite zebrafish embryo has two basic compartments composed of a multicellular blastoderm and a large yolk. In this paper, we determined the volumes of these compartments with light microscopic volumetric measurements; however, the cell concentration in the blastoderm was unknown. Measuring the concentration of cells and the number of the embryos in the samples proved difficult for a number of reasons, including: (1) large size of the embryo produced sample packing problems, (2) low number of samples resulted in poor statistics, and (3) tendency of the embryos to settle in the sample tube. Finally, there was a known permeability barrier to some chemicals within the zebrafish embryo (Hagedorn et al., '96). Therefore, to calculate the intracellular water volume, it was necessary to determine whether tempone was able to freely permeate into all the compartments.

To overcome these problems, we used magnetic resonance (MR) microscopy to determine the extent of tempone permeation in the compartments and devised an ESR technique that does not require knowledge of the cell or embryo concentration in the sample.

METHODS AND RESULTS

Sample preparation

The details of sample preparation have been described in the main body of the paper.

MR microscopy

Because paramagnetic spin labels are NMR relaxation (or contrast) agents (Koutcher et al., '84), an elegant solution to the tempone permeability problem presented itself. MR microscopy, which

has previously been successfully applied to the zebrafish embryo (Hagedorn et al., '96), was used to map $1/T_2$ relaxation rates in the yolk and blastoderm portions of the zebrafish embryo in the presence and absence of 250 mM tempone bathing medium (details presented earlier in this paper). Those compartments into which tempone permeated exhibited enhanced proton relaxation (higher $1/T_2$ rate) when compared with control rates without tempone. The results of this study demonstrated that tempone did not penetrate the yolk compartment of the zebrafish embryo (control rate in the yolk = 97.7 ± 3.1 SEM 1/sec; experimental rate in the yolk = 89.6 ± 7.3 SEM 1/sec). This is both an advantage and a disadvantage in that ESR is able to sample specific subcellular compartments, but not able to determine the total intracellular water of the system.

ESR

Our key modification to the standard ESR methodology takes advantage of the CrOx-broadened extracellular signal to measure the volume of the extracellular medium concurrently with the measurement of intracellular water. The zebrafish embryo samples can be considered to consist of three compartments: (1) tempone-accessible extracellular (water) volume, (2) tempone-accessible intracellular water volume, and (3) tempone-inaccessible intracellular volume. The first and second of these quantities were measured, allowing the third to be computed. Using the last two of these quantities, the fraction of tempone-accessible water in the embryo was computed.

As frequently happens in ESR studies, reduction of the spin label caused a slow exponential decay of the ESR signal (Haak et al., '76; Eriksson et al., '86). This was corrected for by using standard techniques, as described below. Additionally, sample settling occurred during the measurements, and the means for dealing with this are also outlined below.

ESR procedures and analysis

A typical ESR spectrum of zebrafish embryo equilibrated in embryo medium (EM) containing 2 mM tempone and 9.1 mM CrOx is illustrated in Figure 1A. A narrow line reference standard, containing EM and 2 mM tempone, is prepared and measured using the same procedures, samples tubes, and spectrometer configuration/settings as the zebrafish embryo samples. A broad line reference standard (Fig. 1B) containing EM, 2 mM tempone, and 9.1 mM CrOx is prepared and mea-

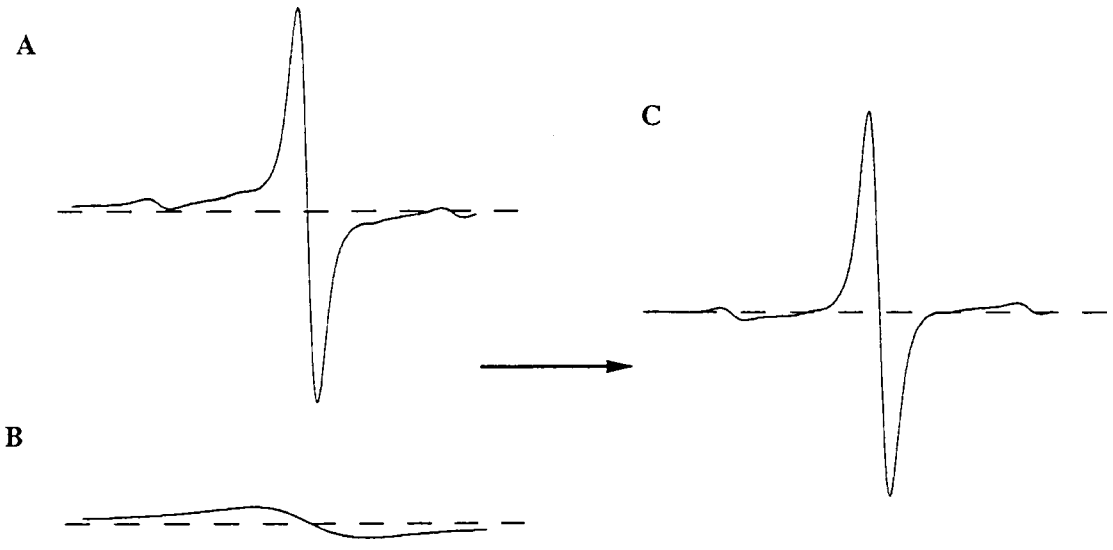

Fig. 1. ESR spectra of a zebrafish embryo sample showing decomposition into intra- and extracellular components. Only the center line of the tempone triplet is shown. The small satellite peaks to the left and right of the center peak are superhyperfine splitting peaks due to the natural abundance of the ^{13}C, and do not interfere with the central peak. **A**: Zebrafish embryo sample (cytocrit ≈ 50%) labeled with 2 mM tempone and 9.1 mM CrOx showing the composite broad extracellular and narrow intracellular signal. **B**: The CrOx-broadened reference standard (EM, 2 mM tempone and 9.1 mM CrOx) scaled to match the broad line component in 1A. Although the scaled broad line component is low in height (h), it represents a significant fraction of the total intensity ($I = w^2h$) where (w) is the peak-to-peak width of the line. **C:** Intracellular water signal of zebrafish embryo sample obtained by the digital subtraction of the spectra C = A – B.

sured similarly. The broad line standard is scaled so that, upon subtraction from the zebrafish embryo spectrum, the extracellular background component is removed, leaving a narrow line intracellular signal (Fig. 1C). The end point for this scaling and subtraction process occurs when the resulting narrow line signal has an essentially flat baseline. The scaled broad line standard is used as a proxy for the extracellular component of the zebrafish embryo signal.

Spectral intensities of the varoius signals were computed using the conventional approximation, $I = w^2h$, where w and h are the spectral peak-to-peak line width and height, respectively, of a first derivative spectrum (Wertz and Bolton, '72). All measurements were made on the middle field line of the tempone triplet.

Correction for signal decay and sample settling

Two characteristics of the zebrafish embryo complicate the analysis of intracellular water volume. First, the tempone nitroxyl radical is reduced by cytoplasmic factors (Eriksson et al., '86). The degradation of tempone does not significantly affect the analysis when a large excess of extracellular tempone is present. However, in our ESR experiments, the reservoir of extracellular solution was insufficient to prevent a gradual loss of ESR signal over the 30-min measurement periods. The second complicating factor was the gradual settling of embryos in the ESR capillary during the experiment. The combined effect of these factors is illustrated in a typical experiment shown in Figure 2. ESR spectra taken between 420 and 1260 sec after embryos were placed into the sample capillary exhibit a decreasing spectral intensity. At the shortest times (420 and 540 sec), the intensity was affected by settling of the embryos which increased the concentration of the embryos within the active sample region. At longer times, an exponential decrease in spectral intensity was observed, due to reduction of the tempone. Exponential signal decay can be described as follows:

$$h(t) = h_o \exp(-t/\tau_c) \quad (1)$$

where $h(t)$ and h_o are the spectral heights at time (t) and time zero, respectively, and τ_c is the decay time constant. Decay times averaged 21 minutes and were individually determined for each zebrafish embryo sample from the postsettling points. These

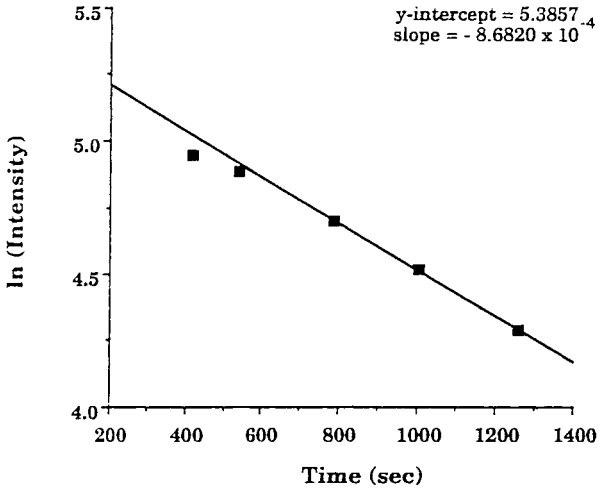

Fig. 2. Typical zebrafish embryo sample illustrating the decay in ESR signal intensity ($I = w^2h$) of the middle field tempone line as a function of time. The first two points are low because the sample is still settling and increasing in embryo concentration. The final three points exhibit clean, exponential decay.

decay times were used to correct the spectral intensities of the first measured spectrum in each series back to t = 0 when the (unreduced) tempone concentration is 2 mM. In effect then, the samples are analyzed at a cell concentration given by the first time point, but with intensities corrected to 2 mM tempone concentration.

Fractional volumes

Determining the fraction of tempone-accessible water in zebrafish embryo is a two step process. First it is necessary to caluclate the fractional volumes of the three components of the zebrafish embryo sample relative to the entire sample volume. These are: (1) the tempone-accessible, extracellular fraction, f_e; (2) the tempone-accessible, intracellular water fraction, f_w; and (3) the tempone-inaccessible, intracellular fraction, f_b. Following standard ESR methodology and assumptions (see previously cited references and the example in the introduction), the first two are given by:

$$f_e = I_e/I_{bs} \quad (2)$$

and

$$f_w = I_w/I_{ns} \quad (3)$$

where I_e and I_w are the intensities of the extracellular (proxy) and intracellular zebrafish embryo signals, respectively. I_{bs} and I_{ns} are the intensity

of the broad line and narrow line reference standards, respectively.

To compute f_b we note that the fractional sample volumes add to one:

$$f_e + f_w + f_b = 1 \quad (4)$$

and thus

$$f_b = 1 - f_e - f_w. \quad (5)$$

Finally, it is the characteristics of the zebrafish embryo that we are interested in, and not the entire ESR sample. The fractional volume of tempone-accessible water in the zebrafish embryo (F_w), is given by:

$$F_w = f_w/(f_w + f_b). \quad (6)$$

Typical numbers for the various fractional quantities are as follows: $f_w = 0.18$; $f_b = 0.38$; $f_e = 0.44$; and $F_w = 0.32$. Thus, the zebrafish embryo occupied 56% of the ESR sample volume, and 32% of the zebrafish embryo was tempone-accessible water. Considering that the blastoderm constitutes ca. 39% of the embryo volume at this developmental stage, this yields a value 82% water in the blastoderm compartment.

In summary, we outlined an ESR and MR methodology for the measurement of fractional, intracellular water volume in situations where tempone does not fully permeate the cell and/or where cell concentration cannot be readily measured. These techniques may be applicable to measurement of intracellular water fractions in other complex, multicompartmental systems, such as tissues and organs.

LITERATURE CITED

Eriksson, U.G., T.N. Tozer, G. Sosnovsky, J. Lukszo, and R.C. Brasch (1986) Human erythrocyte membrane permeability and nitroxyl spin-label reduction. J. Pharm. Sci., *75*: 334–337.

Haak, R.A., F.W. Kleinhans, and S. Ochs (1976) The viscosity of mammalian nerve axoplasm measured by electron spin resonance. J. Physiol., *263*:115–137.

Hagedorn, M., E. Hsu, U. Pilatus, D.E. Wildt, W.F. Rall, and S.J. Blackband (1996) Magnetic resonance microscopy and spectroscopy reveal kinetics of cryoprotectant permeation in a multicompartmental biological system. Proc. Natl. Acad. Sci. *93*:7454–7459.

Hammerstedt, R.H., A.D. Keith, W. Snipes, R.P. Amann, D. Arruda, and L.C. Greil (1978) Use of spin labels to evaluate effects of cold shock and osmolality on sperm. Biol. Reprod., *18*:686–696.

Kleinhans, F.W., V.S. Travis, J. Du, P.M. Villines, K.E. Colvin, and J.K. Critser (1992) Measurement of human sperm intracellular water volume by electron spin resonance. J. Androl., *13*:498–506.

Koutcher, J.A., C.T. Burt, R.B. Lauffer, and T.J. Brady (1984) Contrast agents and spectroscopic probes in NMR. J. Nucl. Med., *25*:506–513.

Moronne, M.M., R.J. Mehlhorn, M.P. Miller, L.C. Ackerson, and R.I. Macey (1990) ESR measurements of time-dependent and equilibrium volumes in red cells. J. Membr. Biol., *115*:31–40.

Vistnes, A.I., and J.S. Puskin (1981) A spin label method for measuring internal volumes in liposomes or cells, applied to Ca-dependent fusion of negatively charged vesicles. Biochem. et Biophys. Acta, *644*:244–250.

Wertz, J.E., and J.R. Bolton (1972) Electron Spin Resonance: Elementary Theory and Practical Applications. McGraw-Hill, New York.